(GODDARD) GRANT - IN

90

The Catholic University of America
Washington, D.C. 20064

80198 CR

25P.

FINAL REPORT

Grant no: NAG 5-792

Submitted to: Laboratory for Extraterrestrial Physics
Goddard Space Flight Center
National Aeronautics and Space Administration
Greenbelt, Maryland 20771

Title: STREAM STRUCTURES IN THE OUTER HELIOSPHERE

Date: July 15, 1987

N87-25139

(NASA-CR-180429) STREAM STRUCTURES IN THE OUTER HELIOSPHERE Final Report (Catholic Univ. of America) 25 p Avail: NTIS HC A02/MF A01 CSCL 03B G3/90 Unclas 0080198

Principal Investigator: Y. C. Whang

Y. C. Whang, Professor
Dept. Mechanical Engineering
Catholic University of America
Tel: 202-635-5170

ADMINISTRATIVE ASPECT

This grant supported a research associate (Professor Gongliang Zhang) to work for Dr Burlaga of NASA Goddard Space Flight Center for a three-month period from December 1, 1986 through February 28, 1987. The Catholic University provided the office space, office computer, staff and administrative support for the project. The principal investigator (Y. C. Whang) played the liaison role between GSFC and the University and occasionally provided scientific advice to the research associate.

SCIENTIFIC RESULT

During the three-month period, Zhang and Burlaga studied a problem entitled "magnetic clouds, geomagnetic disturbances,and cosmic ray decreases".

Twenty one magnetic clouds are identified in the years from 1978 through 1984 and studied by the superposed epoch method. The magnetic fluctuations are enhanced ahead of the clouds. While the ratios of the magnetic pressure to the thermal pressure are enhanced in the clouds, the changes of magnetic field intensity and the proton density for clouds preceded by shock are similar to those for clouds that are not preceded by a shock. Strong magnetic field intensities and low proton temperatures are observed in the clouds, and high densities are observed ahead of the clouds. The magnitude of change in Dst index for the case when the southward fields arrive first is comparable to that for the case of northward fields arrive first, and the phase is such that geomagnetic activity is associated with the southward fields. The clouds with an interplanetary shock produce both larger geomagnetic disturbances and greater decreases in the cosmic ray intensity than the clouds without a shock. The decrease in cosmic ray intensity is caused by the turbulent sheath behind an interplanetary shock, but not by a magnetic cloud.

A paper describing the scientific result has been presented at the 1987 Spring Meeting of American Geophysical Union, with the abstract published in EOS. The full paper has been published as an LEP document and is submitted to the Journal of Geophysical Research for publication. A copy of the report is enclosed.

Abstract

Nineteen magnetic clouds are identified in the years from 1978 through 1982 and studied by the superposed epoch method. The magnetic fluctuations, density and temperature are enhanced ahead of the clouds preceded by shocks. Strong magnetic field intensities and low proton temperatures are observed in the clouds. A relatively large (2.5%) decrease in cosmic ray intensity is caused by the turbulent sheath behind an interplanetary shock ahead of a magnetic cloud. Only a small (0.5%) decrease in intensity is associated with the magnetic cloud itself. Magnetic clouds can produce geomagnetic activity with a decrease in the Dst index of the order of 100 gammas. The magnitude of the change in Dst index for the case when southward fields arrive first is comparable to that for the case of northward fields first, and the phase is such that geomagnetic activity is associated with the southward fields.

1. Introduction

A magnetic cloud is a structure whose size is of the order of 0.25 AU at 1 AU in which the magnetic field intensity is high, the magnetic field direction changes smoothly through a large angle, and where the variability of the field, the temperature and the plasma $\beta = NkT/(B^2/8\pi)$ are low (Burlaga et al, 1981). Studies of the statistical properties, and radial evolution of magnetic clouds were reviewed by Burlaga [1984]. Two magnetic clouds were identified with coronal mass ejections by Burlaga et al. [1982], and Wilson and Hildner [1986] found additional support for the identification of magnetic clouds with coronal mass ejections.

Burlaga et al. [1981] noted that the magnetic cloud which they studied was associated with a geomagnetic storm. The activity began with the arrival of a shock, continued during the passage of that part of the magnetic cloud in which the magnetic field was directed southward, and ended when the magnetic field turned northward in the middle of the magnetic cloud. Wilson [1987] found an association between magnetic clouds and geomagnetic storms at Earth with > 99% confidence.

Cocconi et al. [1958] and Gold [1959,1962] suggested that a tongue-like structure with strong, smoothly varying magnetic fields might produce a decrease in cosmic ray intensity. The magnetic cloud identified by Burlaga et al. [1981] was associated with a decrease in cosmic ray intensity, beginning with the arrival of the shock, but the minimum intensity occurred before the arrival of the magnetic cloud. Burlaga et al. [1985] observed that the cosmic ray intensity did not decrease further during the passage of a magnetic cloud seen in the outer heliosphere. On the other hand, Badruddin [1985] reported a possible correlation between magnetic clouds and cosmic ray decreases. Kudo et al. [1985] observed an increase in cosmic ray intensity related to a decrease in the geomagnetic

Dst index, and Iucci et al. [1985] found short-term cosmic ray intensity increases associated with magnetic clouds. A cosmic ray intensity increase was attributed to the depression of cosmic ray cutoff rigidity produced by the ring current during a geomagnetic storm. Clearly the relation between magnetic clouds and cosmic rays is complex and merits further study.

The excellent ISEE-3 observations of the solar wind from 1978 to 1982 provide an opportunity to study magnetic clouds near solar maximum. Using observations from the magnetic field experiment of Smith and from the plasma experiments of Bame and Bridge on ISEE-3, provided by the NSSDC, we identified nineteen magnetic clouds. The aim of this paper is to describe the effects of these magnetic clouds on geomagnetic activity as measured by the Dst index and on the cosmic ray intensity detected by the Deep River NM-64 neutron monitor on earth. The Dst values were provided by the NSSDC, and the Deep River cosmic ray data were obtained from the National Geophysical Data Center, NOAA.

2. Classification of Magnetic Clouds

In this study a solar wind structure is identified as a magnetic cloud if the magnetic field direction changes continuously through a large angle from a large northern (southern) direction to a large northern (southern) direction in a time interval of the order of a day and if the magnetic field intensity is higher than average. (The restriction to north-south variations is made for historical reasons; it is not an essential feature of magnetic clouds.) These structures have relatively low proton temperatures and low beta-values, as is characteristic of the magnetic clouds reported previously. Nineteen magnetic clouds were selected from 1978 through 1982 (see Table 1). A magnetic clouds is called a "positive cloud" if the magnetic field is directed northward when the cloud arrives at the spacecraft and a "negative cloud" if the magnetic

field is first directed southward. This distinction is important for correlations of magnetic clouds with geomagnetic activity. The magnetic clouds are divided into four classes as follows: Class 1, negative cloud preceded by a shock; class 2, positive cloud preceded by a shock; class 3, negative cloud without a shock; and class 4, positive cloud without a shock. The onset time of a magnetic cloud is defined as the time of the first extreme of a monotonic rotation of the magnetic field, and the end time is the time of the other extreme of the rotation. Table 1 shows the class of each magnetic cloud as well as its start time and end time. The table also gives the time of the shock for those clouds which were preceded by a shock. Fifteen of the nineteen magnetic clouds were preceded by a shock (79%), and all but one of the shock-associated clouds was negative (class 1). Six of the magnetic clouds were positive clouds, of which three were shock-associated and three were not shock-associated.

3. Magnetic Clouds and Cosmic Ray Intensity Decreases

We shall examine the relations between the cosmic ray intensity and the magnetic clouds using the superposed-epoch method. Since the cosmic rays respond in the same way to positive and negative clouds, we consider only two sets of magnetic clouds in relation to cosmic rays: those associated with shocks and those not associated with shocks.

The relation between the magnetic clouds and the cosmic ray intensity is shown by the superposed epoch plots in Figure 1 for the cases of magnetic clouds with and without shocks. The cosmic ray intensity is shown as the percentage counting rate of the Deep River NM-64 neutron monitor, I, versus time. A relatively large decrease in the cosmic ray intensity accompanies the passage of the magnetic clouds preceded by a shock, whereas only a small (but still significant) decrease in cosmic ray intensity was associated with the magnetic clouds

that were not preceded by a shock. Thus, a magnetic cloud alone is not very effective in modulating cosmic rays, but a magnetic cloud which drives a shock does produce a relatively large depression in the cosmic ray intensity. The decrease in cosmic ray intensity occurs primarily during the passage of the sheath between the shock and the magnetic cloud. Figure 1 shows that the rms of the magnetic field, σ_c, is high in the sheath and relatively low in the magnetic cloud, suggesting that the cosmic rays are mainly modulated by scattering from magnetic field fluctuations rather than by drifting in the strong, smooth fields in the magnetic cloud.

The recovery of the cosmic ray intensity for the events associated with shocks begins during the passage of the magnetic cloud, several hours after the cloud arrives at the spacecraft (see Figure 1). The cosmic ray intensity is still depressed even after the magnetic cloud has passed the spacecraft, indicating again that the magnetic cloud is not the principal cause of the decrease in cosmic ray intensity for this class of events. The recovery is evidently a non-local phenomenon, probably associated with the outgoing shock and the turbulent sheath.

Superposed epoch plots of the bulk speed V, proton density N_p and the proton temperature T_p for the events used to construct Figure 1 are shown in Figure 2. The shock-associated magnetic clouds are preceded by a region of approximately 15 hours duration in which the speed, density and temperature are distinctly higher than elsewhere in the vicinity of the magnetic clouds. No such enhancements are observed ahead of the magnetic clouds which are not preceded by a shock.

4. Magnetic Clouds and Geomagnetic Disturbances

The correlation between geomagnetic disturbances and interplanetary magnetic clouds was studied by Wilson [1987] for

the period from 1973 through 1978. However, he did not distinguish between positive and negative clouds, and he did not consider the plasma properties of the magnetic clouds. We examine the geomagnetic effects of magnetic clouds from 1978 to 1982. We consider the positive and negative magnetic clouds separately, since the geomagnetic reponse is sensitive to the direction of the magnetic field, and we discuss the plasma parameters for the two classes of magnetic clouds.

Superposed epoch plots of the magnetic field strength, the latitude angle of the magnetic field and the Dst index for positive and negative clouds are shown in Figure 3. The magnetic field strength profile for the positive clouds is very similar to that for the negative clouds, and the magnitude of the maximum latitude is approximately 70° in both cases. The magnetic field is directed southward at the time of arrival of the negative clouds and northward at the time of arrival of the positive clouds, since that is how the clouds were classified. The geomagnetic response is different in the two cases. For the negative clouds the Dst index decreased at the time of the arrival of the cloud and increased during the passage of the rear half of the magnetic cloud, whereas for the positive clouds the Dst index did not decrease significantly until the arrival of the middle of the cloud, when the magnetic field turned southward. For both classes of magnetic clouds, the Dst index recovered when the magnetic field turned northward. These results are consistent with the well-known fact that geomagnetic activity is greater when the magnetic field is southward than when it is northward (see Fairfield and Cahill, 1966, and Baker et al., 1983).

The minimum Dst is 125 gammas for the negative clouds and 91 gammas for the positive clouds. The difference cannot be attributed to the strength of the maximum southward component of the magnetic field, which was nearly the same for the two classes of events. Thus, it is likely that the difference in

Dst is related to differences in the plasma parameters for the two classes of magnetic clouds. Figure 4 shows superposed epoch plots of the speed, density and temperature for the two classes of events in Figure 4. Indeed, the speed ahead of the negative clouds happens to be higher than that ahead of the positive clouds. (This may be simply a coincidence rather than an intrinsic property of the two types of magnetic clouds.) Since speed is known to be correlated with geomagnetic activity (see Baker et al., 1984), it is not surprising that we observe a deeper minimum in Dst for the shock-associated magnetic clouds.

5. Typical Events

Here we describe four particular events, one from each of the four classes of events described above, which show the features derived from the statistical study presented above.

A negative cloud (southward magnetic field observed at the arrival of the magnetic cloud) preceded by a shock, the December 17, 1980, event is shown in Figure 5. The maximum magnetic field strength is 34 gammas, the highest field strength in the events listed in Table 1. The latitude angle of the magnetic field increases almost linearly from -67° to 87°, and the fluctuations in the magnetic field direction are greatest between the shock and the magnetic cloud, the maximum rms being approximately 18 gammas. The event produced a large geomagnetic storm with a minimum Dst of -240 gammas, beginning at the onset of the magnetic cloud when θ and B_z were most negative. The cosmic ray intensity decreased 4% during the passage of the turbulent sheath between the shock and the front of the magnetic cloud. The local maximum in intensity observed during the decline is related to a diurnal variation, since it was followed by three other maxima one day apart, and it may be associated with a change in the cutoff rigidity as discussed by Iucci et al. [1985] and Kudo et al. [1985].

A positive cloud (northward magnetic field observed at the arrival of the magnetic cloud) which is preceded by a shock, the March 19, 1980, event is shown in Figure 6. The maximum magnetic field intensity is 16 gammas, and the latitude angle decreases from 83° to -80°. In this case a moderate geomagnetic storm began at the time of passage of the middle of the magnetic cloud, when the magnetic field turned southward. The cosmic ray intensity began to decrease at the time of arrival of the shock and it reached a minimum 19 hours later, but there was a maximum in intensity at the front of the magnetic cloud; this maximum might be a diurnal variation, since it was followed by two similar enhancements with separations of 24 hours.

A negative cloud without a shock, the January 16, 1978, event is shown in Figure 7. In this case, the magnetic field direction rotates from -80° to 50° and back to large negative values, suggesting that the symmetry axis of the magnetic cloud is highly inclined with respect to the ecliptic. The maximum magnetic field intensity is about ten gammas, and the maximum rms is 9 gammas. A moderate decrease in Dst occurs at the time of arrival of the magnetic cloud, and the Dst recovers rapidly when the magnetic field turns northward. A small decrease in cosmic ray intensity occurs at the time of arrival of the magnetic cloud. Thus, although a shock seems to be required to produce a large decrease in cosmic ray intensity, a magnetic cloud without a shock can cause a small decrease in the cosmic ray intensity.

Finally, we illustrate a positive cloud without a shock by the December 3, 1979, event in Figure 8. The latitude angle of the magnetic field vector decreases from 30° to -80° as the magnetic cloud moves past the spacecraft. The maximum magnetic field intensity and the fluctuations in the magnetic field direction are small, suggesting that the spacecraft intercepted the magnetic cloud far from the symmetry axis. The Dst index increases during the passage of the first half of the magnetic

cloud, when the magnetic field is directed northward, and it decreases when the magnetic field turns southward. No appreciable decrease in the cosmic ray intensity is observed in this case, but again there are large diurnal variations that complicate the cosmic ray intensity profile.

Summary

We have identified nineteen magnetic clouds using the plasma and magnetic field data from ISEE-3 for the period from 1978 to 1982, and we examined their effects on the cosmic ray intensity measured by the Deep River NM-64 neutron monitor and on the geomagnetic activity measured by the Dst index. The principal results of our superposed epoch analysis are as follows.

A relatively large (~2.5 %) decrease in the cosmic ray intensity is associated with a magnetic cloud preceded by a shock, and only a small (~0.5%) decrease in the cosmic ray intensity is associated with a magnetic cloud that is not preceded by a shock. The turbulent magnetic fields associated with the sheath between a shock and a magnetic cloud are more effective in modulating the cosmic rays than the strong ordered magnetic fields in a magnetic cloud.

A magnetic cloud produces a geomagnetic storm with a decrease in the Dst index of approximately 100 gammas. The time of onset of the geomagnetic activity coincides with the arrival of the magnetic cloud when the magnetic field is southward in the leading half of the magnetic cloud, and the time of onset of geomagnetic activity occurs approximately at the passage of the midpoint of the magnetic cloud when the magnetic field is northward in the leading half of the magnetic cloud. The change in the Dst index is somewhat greater for clouds with high speeds than for clouds with low speeds.

Acknowledgements

G. Zhang expresses his heartfelt thanks to Drs. N. Ness, Y. C. Whang and W. J. Kelnhofer for their kind invitation and hospitality during his visit at Goddard Space Flight Center and The Catholic University of America. Thanks are due to Dr. L. Klein and members of the Information Analysis and Display Branch of the Laboratory for Extraterrestrial Physics at GSFC for their help. The plasma and magnetic field data for this study are from the tape prepared by Couzens and King, which was provided to us by the NSSDC, and the Deep River neutron monitor data were provided by the NGDC, NOAA.

References

Baker, D. N., S.-I. Akasofu, W. Baumjohann, J. W. Bieber, D. H. Fairfield, E. W. Hones, Jr., B. Mauk, R. L. McPherron, and T. E. Moore, Substorms in the magnetosphere, in Solar Terrestrial Physics: Present and Future, edited by D. M. Butler and K. Papadopoulos, NASA Reference Publication 1120, 1984.

Badruddin, R., S. Yadov, N. R. Yadov, and S. P. Agarawal, Influence of magnetic clouds on cosmic ray intensity variations, Proc. 19th ICRC, SH 5.1-12, 1985.

Burlaga, L. F. MHD processes in the outer heliosphere, Space Science Reviews, 39, 255, 1984.

Burlaga, L. F. E. Sittler, F. Mariani, and R. Schwenn, Magnetic loop behind and interplanetary shock: Voyager, Helios and IMP 8 observations, J. Geophys. Res., 86, 6673, 1981.

Burlaga, L. F., L. Klein, N. R. Sheeley, Jr., D. J. Michels, R. A. Howard, M. J. Koomen, R. Schwenn and H. Rosenbauer, A magnetic cloud and a coronal mass injection, Geophys. Res. Letters, 9, 1317, 1982.

Burlaga, L. F., F. B. Mc Donald, M. L. Goldstein, and A. J. Lazarus, Cosmic ray modulation and turbulent interaction regions near 11 AU, J. Geophys. Res., 90, 12027, 1985.

Cocconi, G., T. Gold, K. Griesen, S. Hayakawa, and P. Morrison, The cosmic ray flare effect, Nuovo Cimento, 8, 161, 1958.

Couzens, D. A., and J. H. King, Interplanetary Medium Data Book-Supplement 3, 1977-1985, NSSDC/WDC-A 86-04, 1986.,

Fairfield, D. H., and L. J. Cahill, Jr., Transition region magnetic field and polar magnetic disturbances, J. Geophys. Res., 71, 155, 1966.

Gold, T., Plasma and magnetic fields in the solar system, J. Geophys. Res., 64, 1665, 1959.

Gold, T., Magnetic storms, Space Science Rev., 1, 100, 1962

Kodo, S., M. Wada and T. Tanskanen, Transient cosmic ray increase associated with a geomagnetic storm, Proc. of the 19th ICRC, SH-5.1-8, 1985.

Iucci, N., M. Parisi, C. Signorini, M. Storini, and G. Villoresi, Anomalous short-term increases in the galactic cosmic ray intensity: Are they related to interplanetary magnetic cloud-like structures?, Proc. of the 19th ICRC, SH 5.1-3, 1985.

Wilson, R. M., Geomagnetic response to magnetic clouds, Planetary Space Science, to appear, 1987.

Wilson, R. M., and E. Hildner, On the association of magnetic clouds with disappearing filaments, J. Geophys. Res., 91, 5867, 1986.

Figure Captions

Fig. 1. Magnetic clouds and cosmic ray decreases. Left panel: magnetic clouds with a shock ahead. Right panel: magnetic clouds without a shock ahead. From the top to the bottom: the changes in the intensity B, the rms of the magnetic field components, and the count rates of the Deep River NM-64 neutron monitor as a function of time. The curves are superposed epoch plots with zero epoch corresponding to the time of arrival of a magnetic cloud.

Fig. 2. Superposed epoch plots of plasma parameters aassociated with magnetic clouds with shocks (left panel) and without shocks (right panel). From top to bottom: solar wind bulk speed V, proton density, N_p and proton temperature, T_p.

Fig. 3. Magnetic clouds and geomagnetic disturbances. Left panel: negative magnetic clouds with the magnetic field turning southward first. Right panel: positive magnetic clouds with the magnetic field turning northward first. From the top to the bottom: the latitude angle θ, the magnetic field strength B, and the Dst index. The curves are superposed epoch plots with zero epoch equal to the time of arrival of the magnetic cloud.

Fig. 4. Superposed epoch plots of the speed, density and proton temperature associated with positive magnetic clouds (left panel) and negative magnetic clouds (right panel).

Fig. 5. Magnetic cloud, geomagnetic disturbance and cosmic ray intensity decrease; a typical example for a negative cloud with a shock ahead.

Fig. 6. Magnetic cloud, geomagnetic disturbance and cosmic ray intensity decrease; a typical example for a positive cloud with a shock ahead.

Fig. 7. Magnetic cloud, geomagnetic disturbance and cosmic ray intnsity decrease; a typical example for a positive cloud without a shock.

Fig. 8. Magnetic cloud, geomanetic disturbance and cosmic ray intensity decrease; a typical example for a negative cloud without a shock.

Table 1. List Of Magnetic Clouds (1978-1982)

Shock				Cloud Starts				Cloud Ends				Class*
Y	M	D	H	Y	M	D	H	Y	M	D	H	
1978	01	03	22	1978	01	04	12	1978	01	05	23	1
No Shock				1978	01	16	13	1978	01	17	08	3
								(1978	01	18	05)	
1978	04	02	22	1978	04	03	19	1978	04	04	09	1
1978	06	04	13	1978	06	04	24	1978	06	05	17	1?
1978	08	27	05	1978	08	27	18	1978	08	28	13	2
1978	09	29	04	1978	09	29	10	1978	09	30	03	1
No Shock				1978	10	29	23	1978	10	30	09	4?
								(1978	10	31	12)	
1979	04	03	11	1979	04	03	22	1979	04	04	20	1
1979	09	17	10	1979	09	18	08	1979	09	19	07	1?
								(1979	09	19	23)	
No Shock				1979	12	03	11	1979	12	04	16	4
								(1979	12	05	07)	
1980	02	15	??	1980	02	16	04	1980	02	17	09	1
1980	03	19	07	1980	03	19	16	1980	03	21	19	2
1980	12	11	11	1980	12	11	23	1980	12	13	07	1
1980	12	19	07	1980	12	19	14	1980	12	20	13	1
1981	02	06	13	1981	02	06	19	1981	02	07	09	1
1981	03	05	06	1981	03	05	13	1981	03	06	07	1
1981	09	18	20	1981	09	19	07	1981	09	19	20	1
1982	02	11	16	1982	02	12	03	1982	02	13	21	2
No Shock				1982	09	25	22	1982	09	26	18	4

*Class 1 : Negative Clouds With Shock Association
Class 2 : Positive Clouds With Shock Association
Class 3 : Negative Clouds Without Shock Association
Class 4 : Positive Clouds Without Shock Association

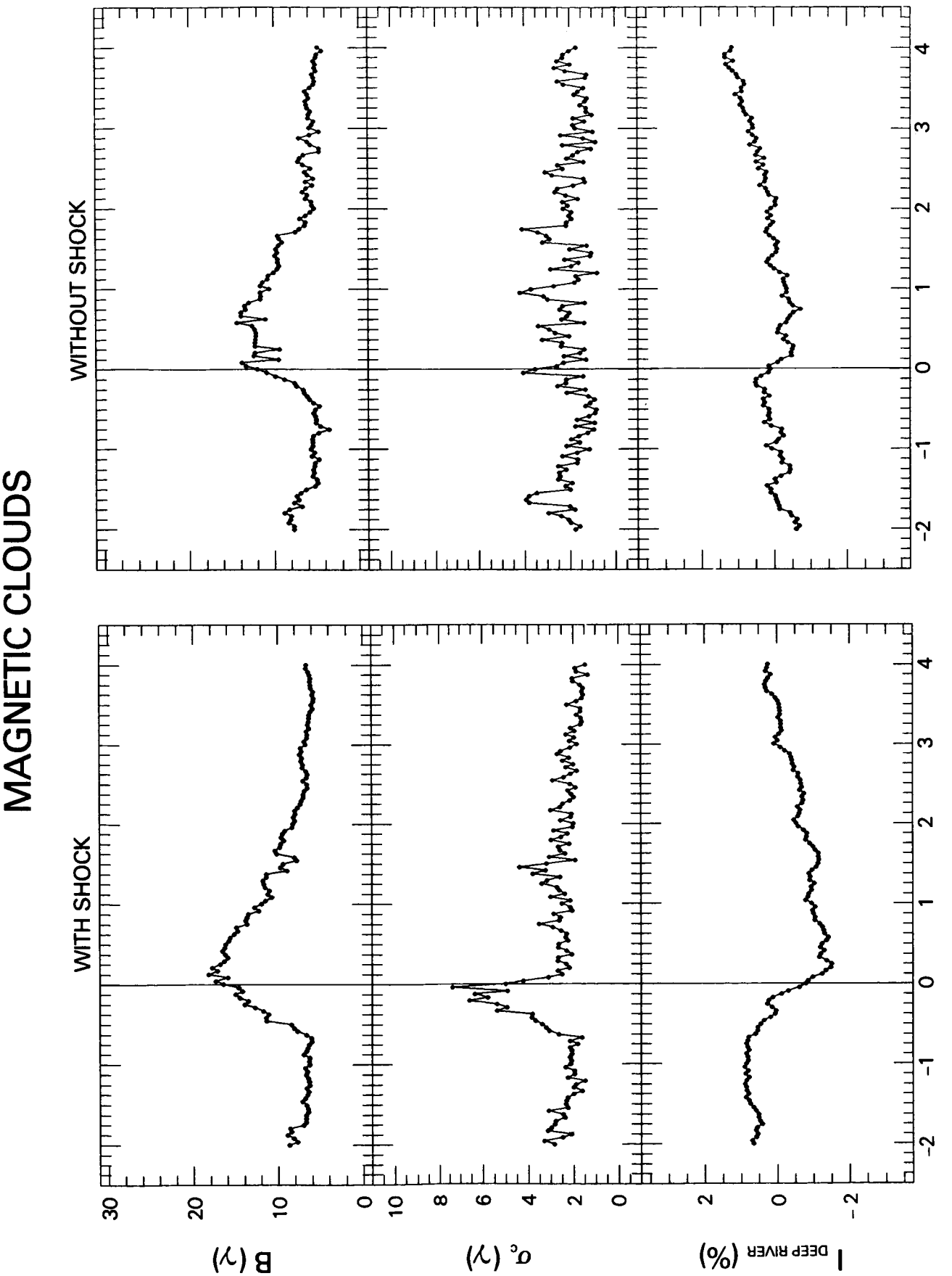
MAGNETIC CLOUDS
WITH SHOCK
WITHOUT SHOCK
B (γ)
σ_c (γ)
I DEEP RIVER (%)
DAYS FROM CLOUD'S START

Figure 1

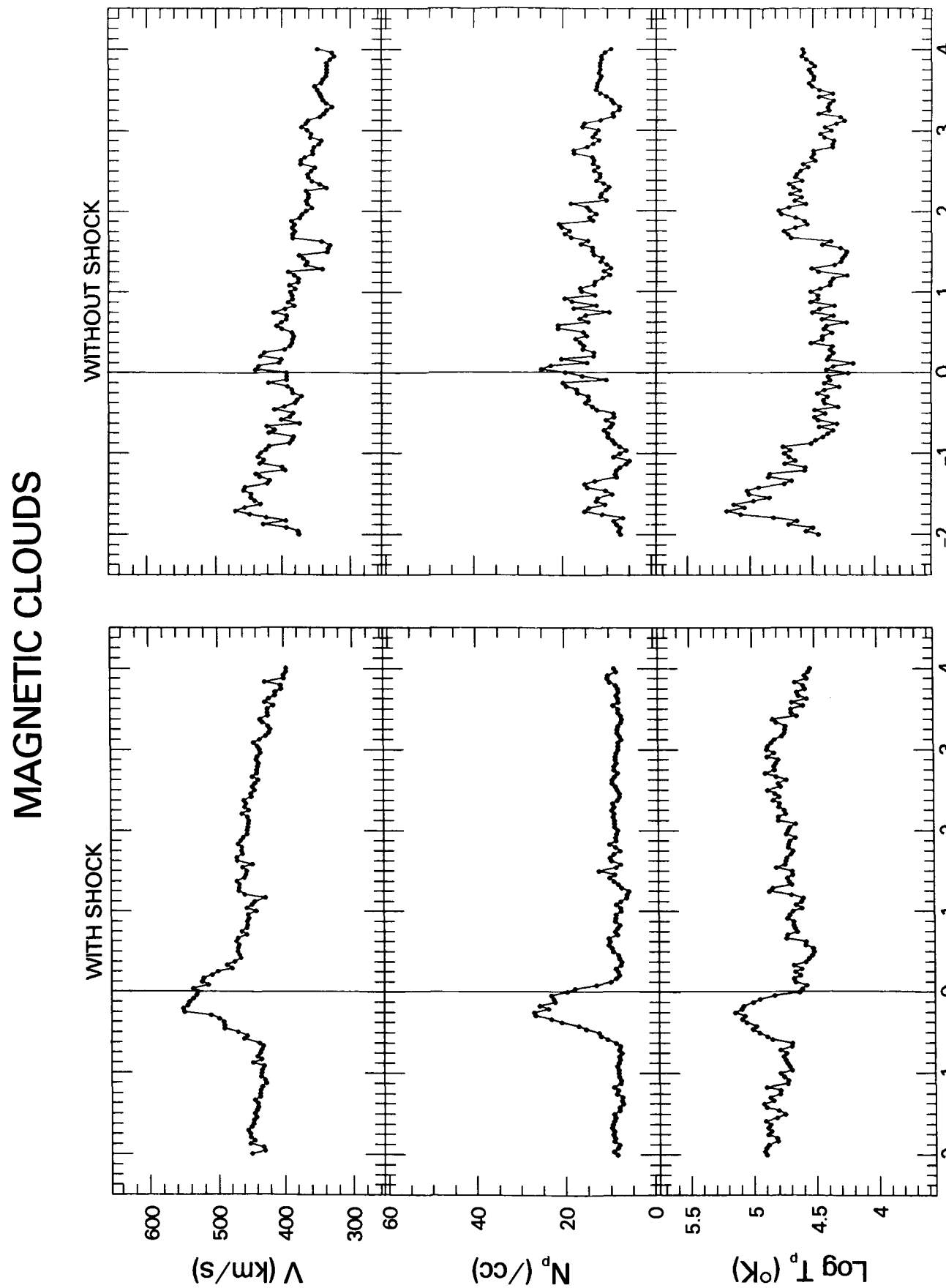
MAGNETIC CLOUDS
WITH SHOCK
WITHOUT SHOCK
V (km/s)
N$_p$ (/cc)
Log T$_p$ (°K)
DAYS FROM CLOUD'S START

Figure 2

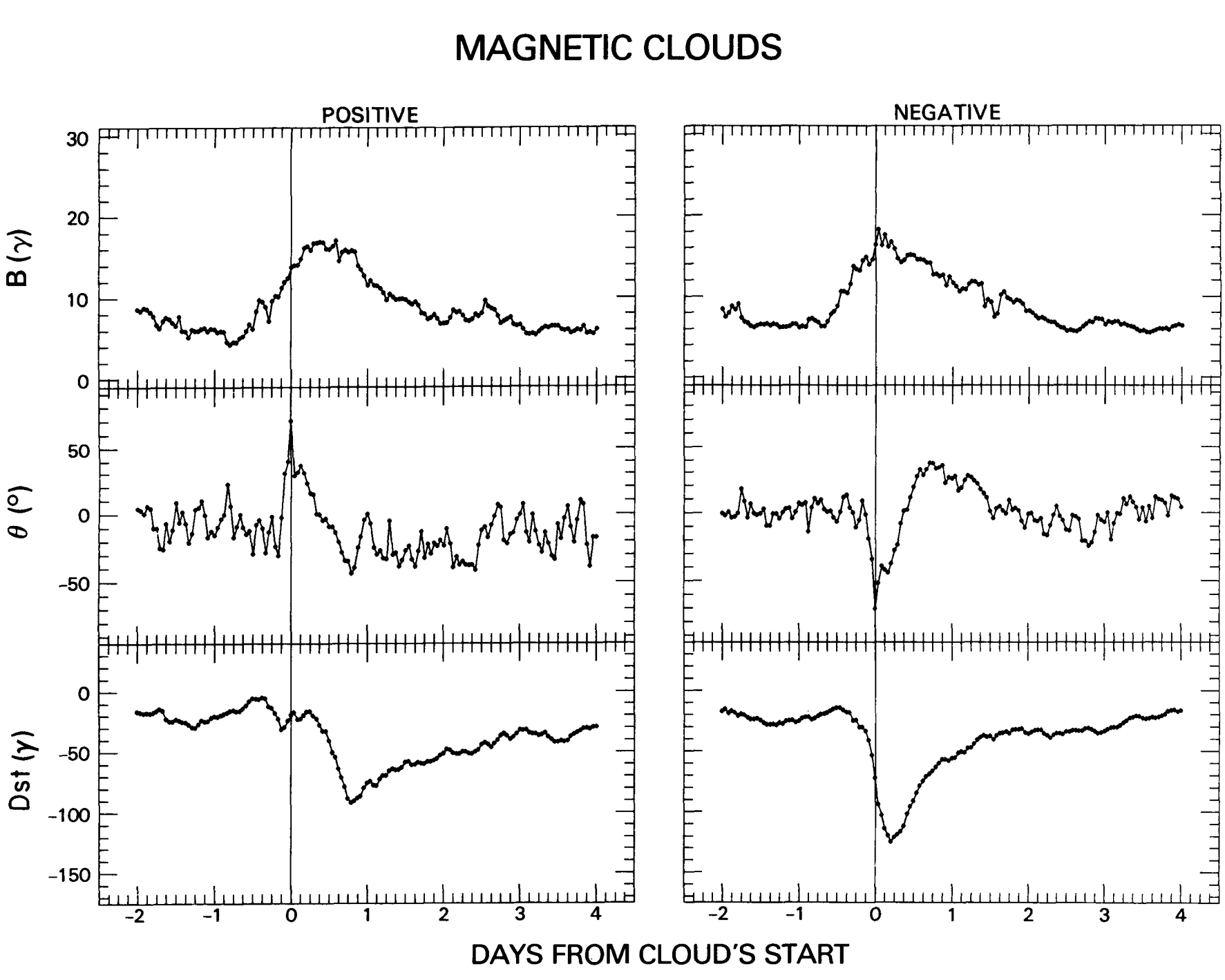
MAGNETIC CLOUDS
POSITIVE
NEGATIVE
B (γ)
θ (°)
Dst (γ)
30
20
10
0
50
0
-50
0
-50
-100
-150
-2
-1
0
1
2
3
4
DAYS FROM CLOUD'S START

Figure 3

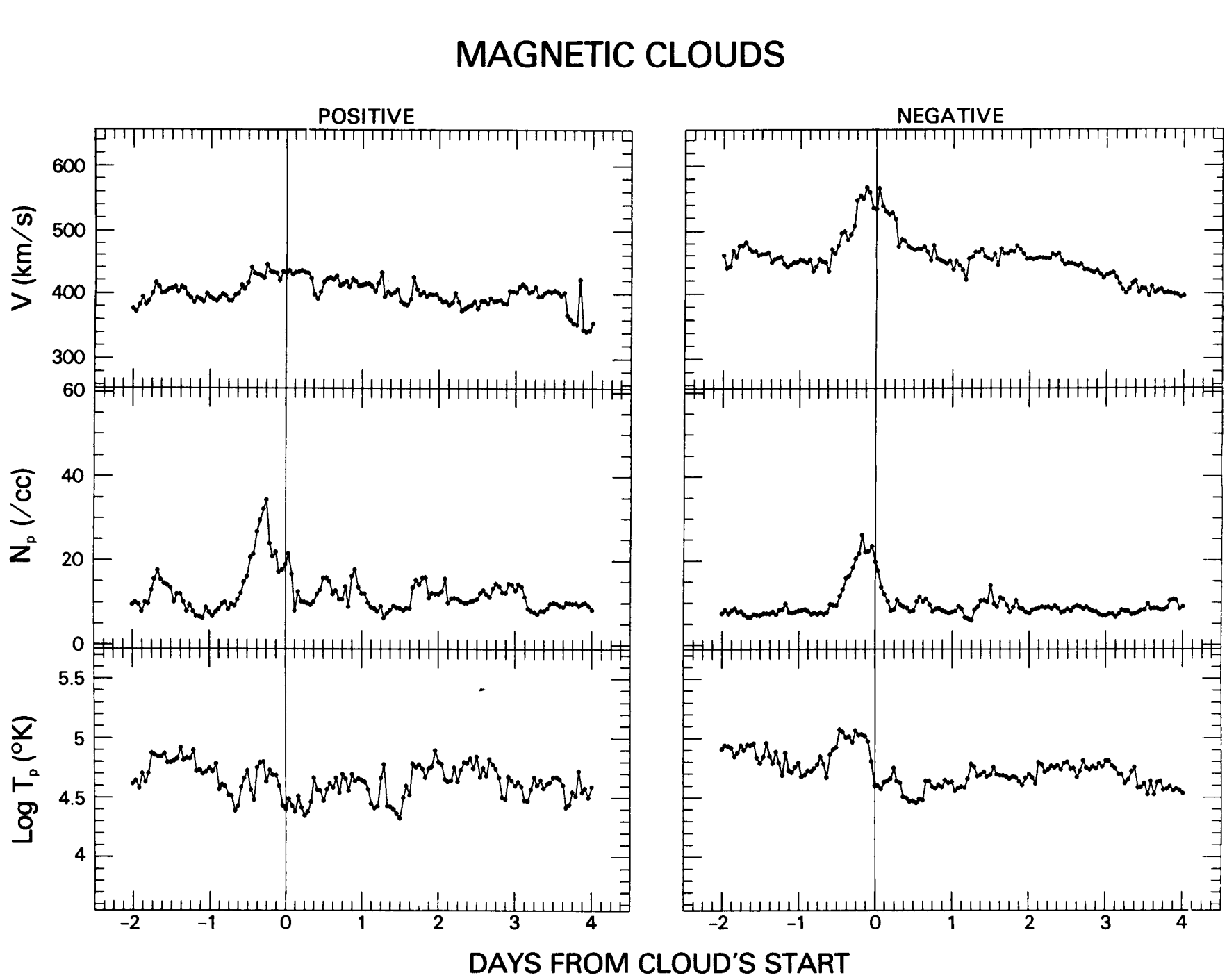
MAGNETIC CLOUDS
POSITIVE
NEGATIVE
V (km/s)
600
500
400
300
60
N_p (/cc)
40
20
0
Log T_p (°K)
5.5
5
4.5
4
-2
-1
0
1
2
3
4
DAYS FROM CLOUD'S START

Figure 4

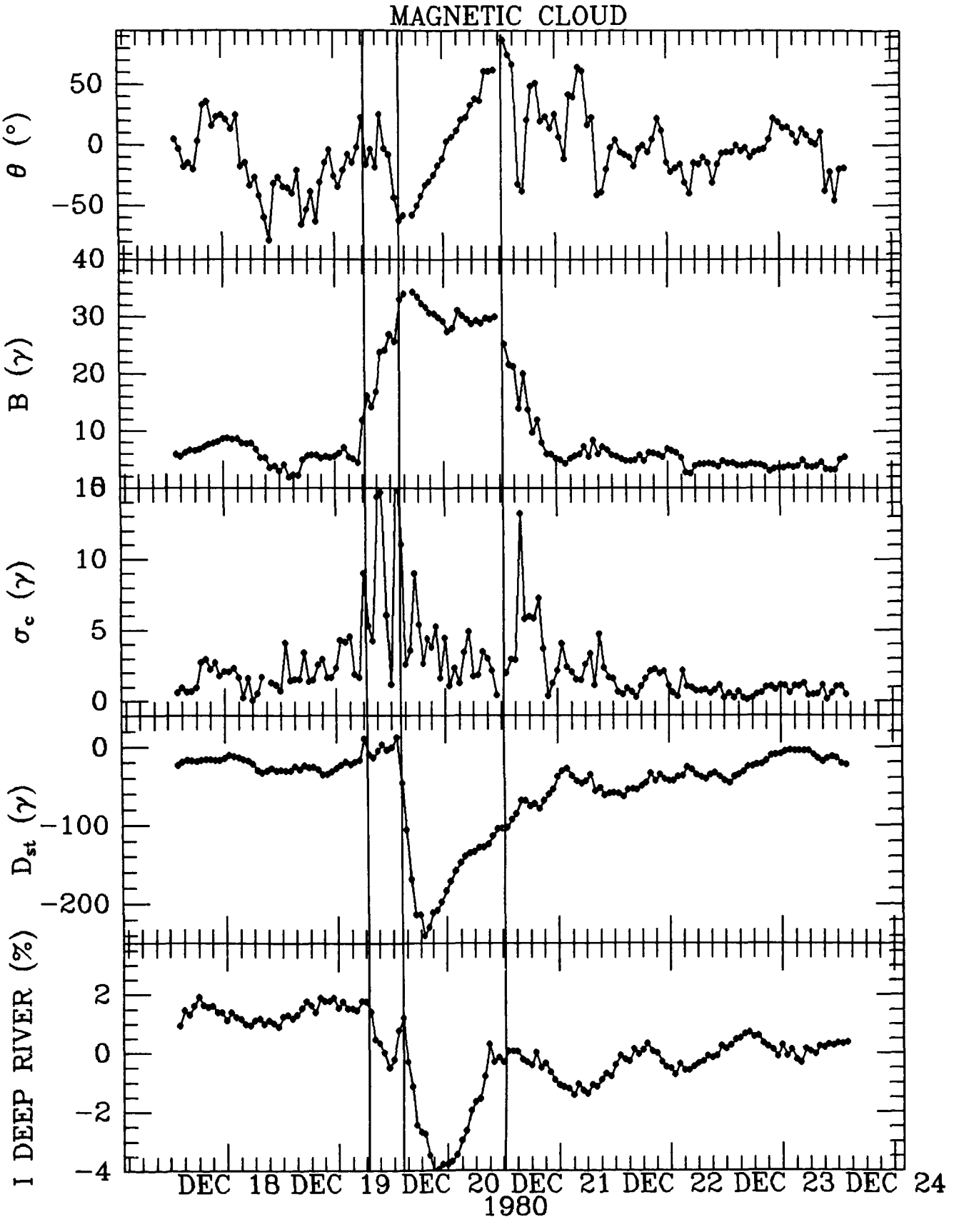
MAGNETIC CLOUD
θ (°)
50
0
−50
B (γ)
40
30
20
10
10
σc (γ)
10
5
0
Dst (γ)
0
−100
−200
I DEEP RIVER (%)
2
0
−2
−4
DEC 18 DEC 19 DEC 20 DEC 21 DEC 22 DEC 23 DEC 24
1980

Figure 5

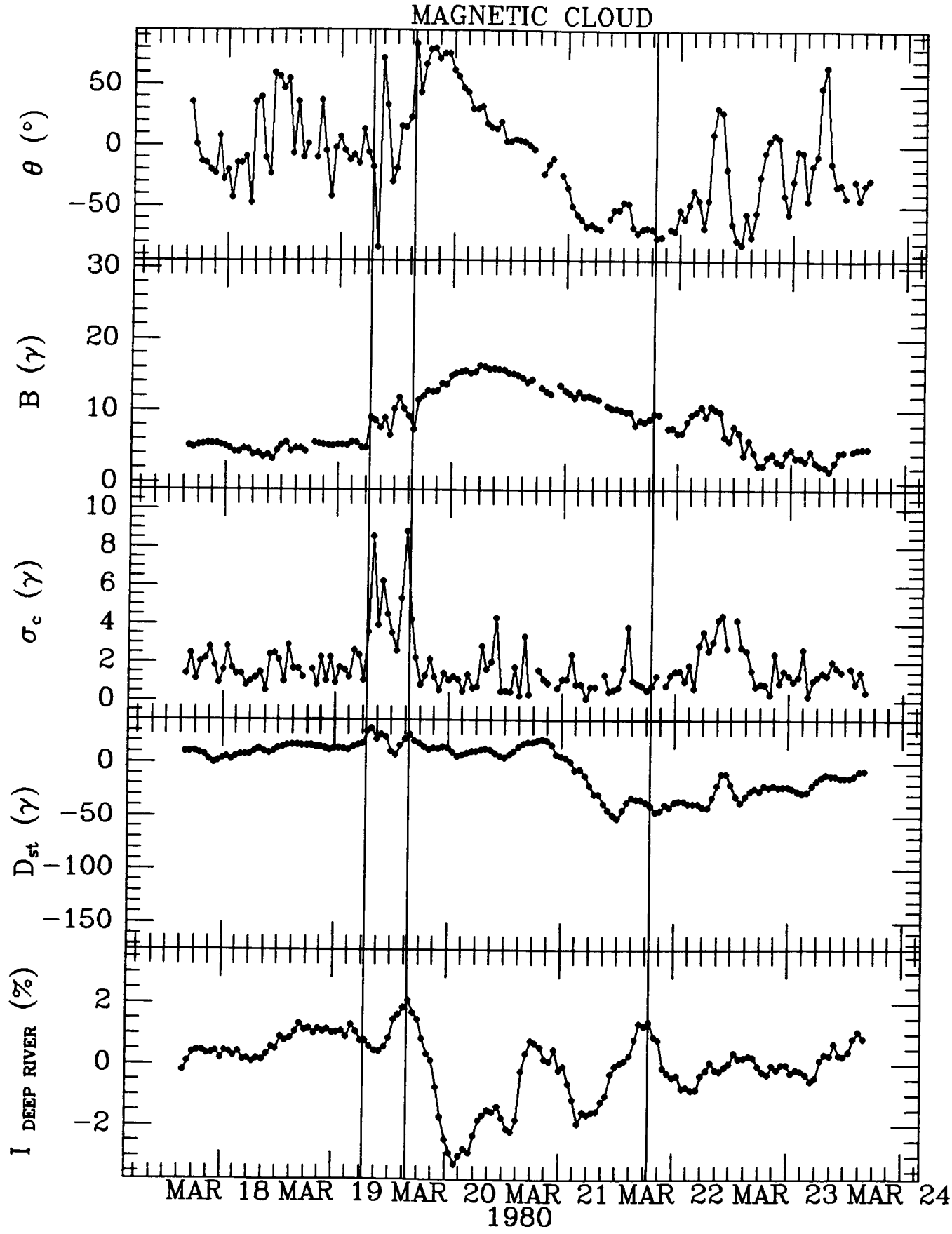
MAGNETIC CLOUD
θ (°)
50
0
−50
30
B (γ)
20
10
0
10
σc (γ)
8
6
4
2
0
0
Dst (γ)
−50
−100
−150
2
I DEEP RIVER (%)
0
−2
MAR 18
MAR 19
MAR 20
MAR 21
MAR 22
MAR 23
MAR 24
1980

Figure 6

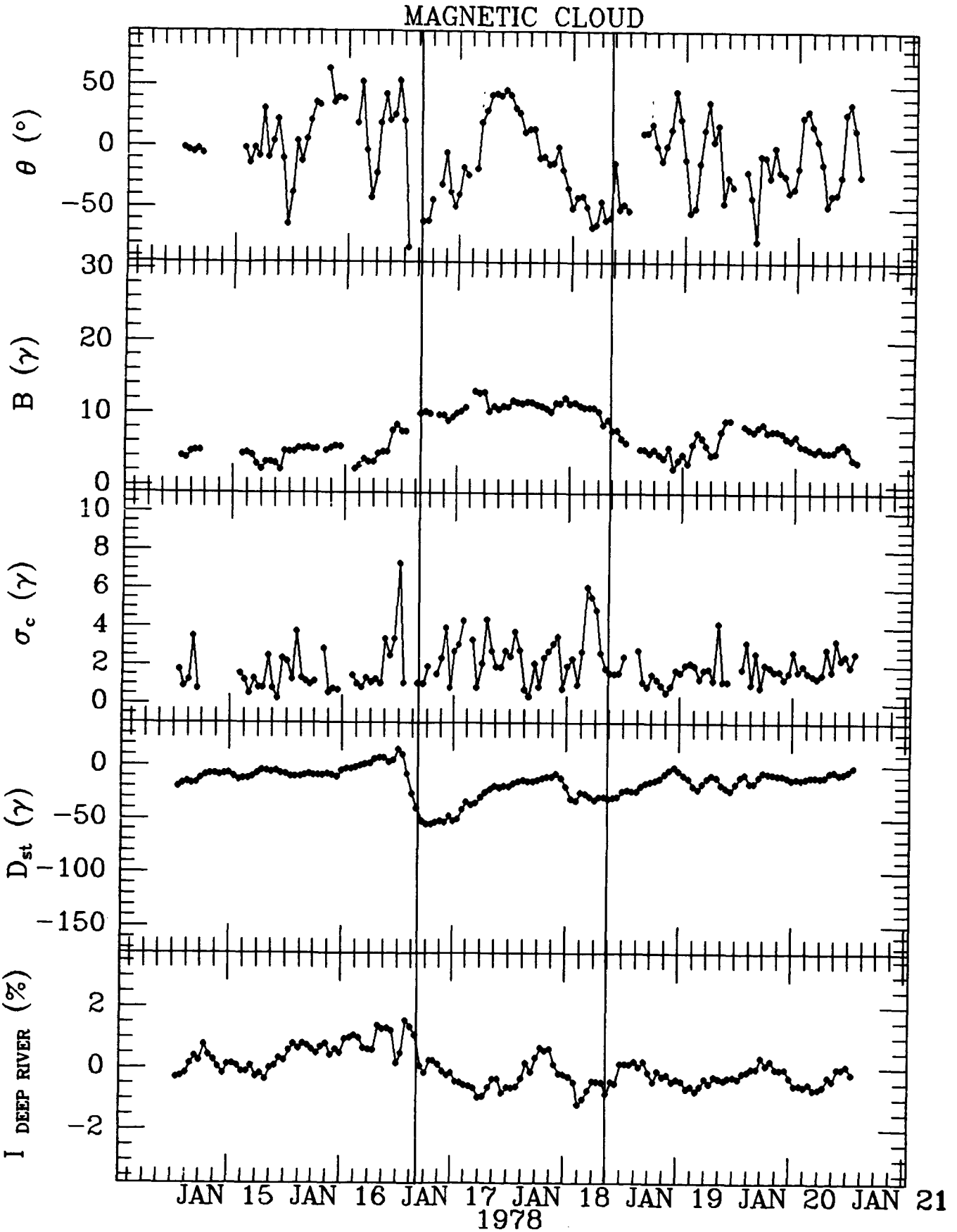
MAGNETIC CLOUD
θ (°)
50
0
−50
B (γ)
30
20
10
0
σc (γ)
10
8
6
4
2
0
Dst (γ)
0
−50
−100
−150
I DEEP RIVER (%)
2
0
−2
JAN 15
JAN 16
JAN 17
JAN 18
JAN 19
JAN 20
JAN 21
1978

Figure 7

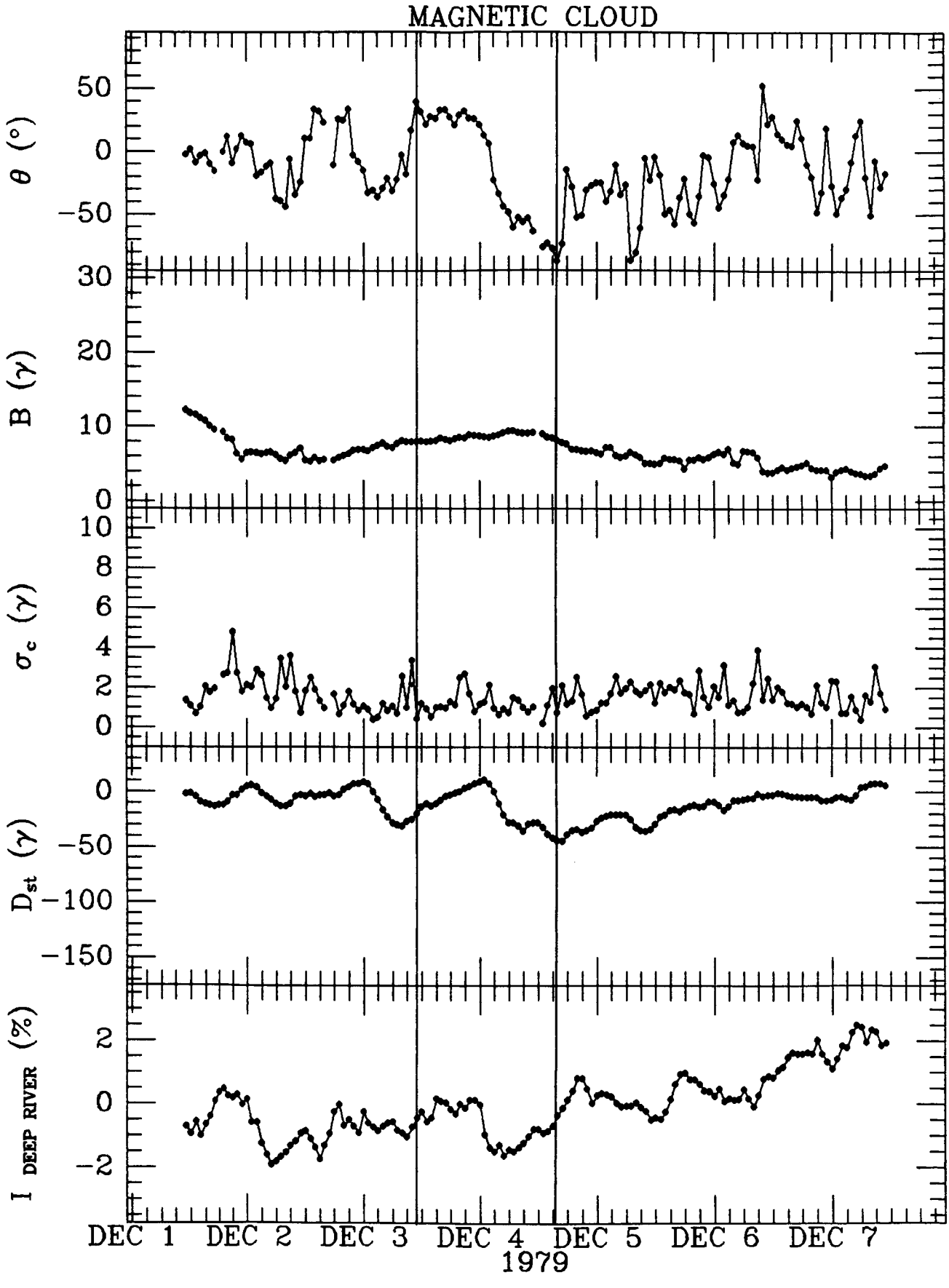
MAGNETIC CLOUD
θ (°)
50
0
−50
B (γ)
30
20
10
0
σc (γ)
10
8
6
4
2
0
Dst (γ)
0
−50
−100
−150
I DEEP RIVER (%)
2
0
−2
DEC 1
DEC 2
DEC 3
DEC 4
DEC 5
DEC 6
DEC 7
1979

Figure 8